

Numerical Computations of Two-Dimensional Unsteady Sprays for Application to Engines

H. C. Gupta* and F. V. Bracco†
Princeton University, Princeton, N.J.

The problem of the numerical computation of the penetration and vaporization of two-dimensional unsteady sprays is considered. This topic is of interest in the field of modeling of combustion in direct injection, internal combustion engines with self-ignition (Diesel), or spark ignition (stratified charge). The spray equation, which is the governing equation and, in this application, exhibits six independent variables, is numerically solved using an upwind difference scheme which is first-order accurate and explicit in time. The problem is set up both as a boundary value problem and an equivalent initial value problem. The boundary value formulation is preferable for applications. A study of the numerical error of the initial value problem is undertaken by comparing the numerical solution with an analytical one. The analytical solution is obtained by discretizing the spray, reducing the spray equation to a set of ordinary differential equations, solving these equations in closed form, and reconstructing the solution for the entire spray by integrating the contributions from the individual, discretized spray parcels. It is concluded that the selected numerical method yields sufficiently accurate results in reasonable computational time. However, the practical usefulness of the model is presently limited due to the simplifying assumptions that were made in order to concentrate on the formulation of the problem, the method of solution, and computational time and accuracy.

Nomenclature

a, b	= constants of the Weber/Reynolds correlation
B	= coefficient in the initial distribution function s^2/cm^7
c	= constant in the Nukiyama-Tanasawa initial distribution function in the drop radius space, cm^{-1}
C_D	= drop drag coefficient
d_1, d_2	= constants in the initial Gauss distribution functions in the velocity space, cm/s
f	= droplet distribution function, s^2/cm^5
F, F_1, F_2	= $(=dv/dt)$ time rate of change of drop velocity following the drop, cm/s^2
h_1, h_2	= constants in the initial Gauss distributions in the physical space, cm
k	= modified vaporization rate constant, g/cm s
p	= pressure, dyn/cm^2
Pr	= gas Prandtl number
r	= radius of the drop, cm
r_{inj}	= injector nozzle radius, cm
r_{30}	= volume-number average radius, cm
R	= time rate of change of drop radius, cm/s
Re	= drop Reynolds number
Re_L	= liquid jet Reynolds number
s	= a coordinate
t	= time, s
Δt	= time step for the numerical integration of the spray equation, s
T	= gas temperature, K
u	= gas velocity, cm/s
v, v_1, v_2	= liquid drop coordinates in the velocity space, cm/s
v_1^*, v_2^*	= centers of the initial Gauss distributions in the velocity space, cm/s
v_{inj}	= liquid injection velocity, cm/s
We	= liquid jet Weber number

\dot{W}_F	= mass rate of injection, g/s
x, x_1, x_2	= liquid drop coordinates in the physical space, cm
x_1^*, x_2^*	= centers of the initial Gauss distributions in the physical space, cm
α	= constant = 0, 1 for planar or cylindrical coordinates
γ	= specific heats ratio
μ	= gas viscosity, g/cm s
μ_L	= liquid viscosity, g/cm s
ξ	= source (or sink) term, s/cm^5
ρ	= gas density, g/cm^3
ρ_c	= condensed-phase density (mass of liquid per unit volume of chamber), g/cm^3
ρ_L	= density of the liquid, g/cm^3
σ_L	= liquid surface tension, dyn/cm
τ_ℓ	= injection time of liquid parcel ℓ , s
$\Delta\tau$	= time step for the numerical evaluation of an integral, s
ϕ	= constant of F in the initial value problem, cm^2/s
χ	= constant of R in the initial value problem, cm^2/s
ψ	= constant = $2\phi + \chi$, cm^2/s

Subscripts

min	= minimum
max	= maximum
0	= parameters used in the initial value problem
i, j, k, l, m	= running indices in finite-difference equations
ℓ	= ℓ th discretized spray

I. Introduction

A SPRAY is formed when a liquid jet or sheet breaks up into small droplets. Since a liquid spray exchanges mass, momentum, and energy with the surrounding gas more rapidly than the original jet or sheet, sprays are employed when the enhancement of such exchange rates is desirable. There are many application of sprays, including spray drying, humidification, chemical processing, fire extinguishment, and fuel injection into combustion chambers. Most of these applications are steady, except for turbulent fluctuations, but some important ones are inherently unsteady.

Simulation of the unsteady sprays, which are found in reciprocating and rotary internal combustion engines, is the

Received March 17, 1978; revision received June 29, 1978.
Copyright © American Institute of Aeronautics and Astronautics, Inc., 1978. All rights reserved.

Index categories: Multiphase Flows; Computational Methods; Combustion and Combustor Designs.

*Graduate Student.

†Associate Professor, Dept. of Aerospace and Mechanical Sciences.
Member AIAA.

ultimate objective of this research. They occur when liquid fuel is injected directly into the compressed air of the combustion chamber, as in compression ignition (Diesel) engines, and in some stratified charge engines. However, the study is of interest also for those of the previously mentioned applications in which steady sprays prevail. Indeed, steady solutions are obtained simply by letting the numerical time variable increase beyond the characteristic time of the unsteady transients through which steady flows establish themselves.

Even though engine flows are generally three-dimensional, two-dimensional schemes, such as those discussed in this paper, constitute reasonable approximations to several engine configurations of practical interest.¹

Several aspects of a multidimensional spray model could be discussed, including physical assumptions and limitations, engineering implications of the results, and the numerical method of solution and its accuracy.

The first two topics are only briefly considered in Sec. II, having been examined in some detail in previous publications.¹⁻⁶ This paper emphasizes the formulation of the problem and its numerical solution, and is organized as follows.

In Sec. III, the fundamental equation of the problem is introduced, some necessary functions are defined, and the difference between thin and thick sprays mentioned. In Sec. IV, two equivalent methods of setting up the problem are identified—the boundary value problem and the initial value problem. The respective initial and boundary conditions are also given. In Sec. V, the upwind differencing scheme used for the solution of both formulations is applied and an equation for the truncation error is given. For practical applications, the boundary value formulation is more convenient. Some results from it are given in Sec. VI. In Secs. VII and VIII, the same physical problem, but in its initial value formulation, is solved both numerically (by the scheme defined in the earlier section) and “analytically” (actually a numerical integration over one independent variable is still employed) and the results are compared to assess the accuracy of the numerical approach. The paper ends with a summary of our conclusions.

II. Description of the Physical Problem and Assumptions

Some two-dimensional combustion chamber configurations for reciprocating and rotary engines are sketched in Fig. 1. In Fig. 1a, the injector is assumed to deliver an axisymmetric spray and the ignition source is assumed to be at the center of the engine head. In Figs. 1b and 1c, the heights of the combustion chambers are assumed to be small (in comparison to the diameter of the cylinder or to the width and length of the rotor) so that consideration of only average properties along these heights is justifiable. Solutions are reported for configuration a, where the motion of the piston was neglected, thus resulting in the fixed volume configuration of Fig. 2.

Normally, injection starts just prior to the combustion chamber achieving its minimum volume and continues after ignition. High injection pressures are used and the resulting high-velocity liquid jets, or sheets, break up into droplets within distances of the order of the injector diameter. This diameter is several orders of magnitude smaller than any chamber dimension and the spray can be assumed to originate, immediately after the beginning of injection, at the injector exit plane itself or from any other reasonably small surface in the vicinity of the injector. Exchanges of mass, momentum, and energy between the spray and the chamber gas start immediately and result in heating and vaporization of the liquid, local cooling of the chamber gas, entrainment of the gas by the liquid, and turbulent mixing of the gases. At some time during the later part of the injection, combustion starts either spontaneously, as in compression ignition engines, or assisted by a spark, as in stratified charge engines.

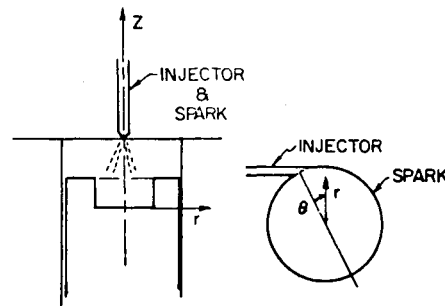


Fig. 1 Some two-dimensional configurations.

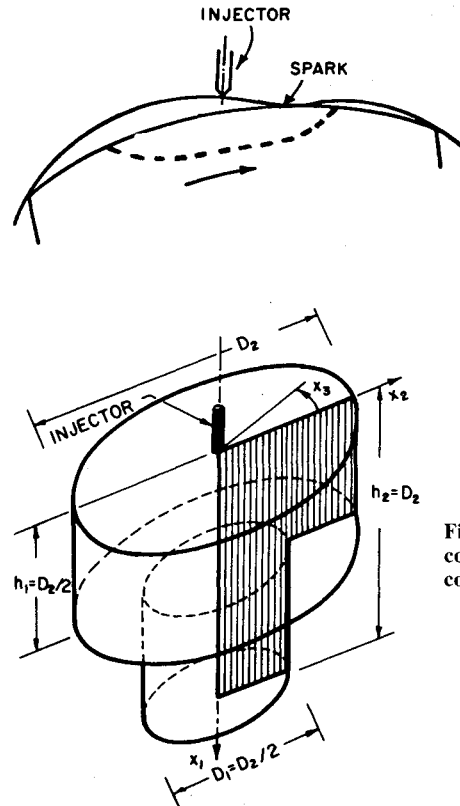


Fig. 2 Chamber and coordinates of the computations.

In early numerical studies of one-dimensional unsteady spray combustion, the two phases were completely coupled through the mass and energy equations, but the force exerted by the liquid on the gas was not accounted for.² First attempts to compute two- and three-dimensional unsteady sprays without combustion are given in Refs. 4 and 5, respectively. Here only one-way coupling was considered in that the drag exerted by the gas on the liquid was accounted for but the gas was totally unaffected by the presence of the liquid. More recently, two-dimensional unsteady engine spray computations have been reported in which the conservation equations for the two phases are fully coupled.⁶

In order to concentrate on the formulation of the problem and the accuracy of the numerical solutions, the physics of the flows studied in this paper is again oversimplified, as in Refs. 4 and 5. Consideration is limited here to the spray prior to ignition, so that no chemical reactions are involved. While considering the spray, the effects of the gas on the spray will be accounted for but the effects of the spray on the gas will be neglected. Accordingly, the gas maintains its initial conditions throughout the injection, penetration, and vaporization process, and only the equations for the spray need be considered. Moreover, the functions that will be used to represent the vaporization and drag of individual drops originate from studies of individual drops in infinite gaseous media and therefore are applicable to thin sprays, while actual engine sprays are mostly thick.¹ Corresponding functions for thick

sprays are currently unknown, but the numerical techniques studied in this paper would apply to thick sprays as well. Finally, the functions that describe some of the initial and boundary conditions for the spray are also questionable because they attempt to describe the outcome of the atomization process, which in itself is poorly understood.⁷ Accordingly, this study represents only an intermediate step toward the formulation and solution of adequate models for actual applications.

III. Spray Equation

Two sets of conservation equations are currently under investigation to represent spray problems. One procedure depends on the solution of the spray equation⁸ to compute the development of the liquid phase and to provide mass, momentum, and energy source terms for the gas phase conservation equations.²⁻⁶ In the second procedure, the two phases are treated more symmetrically in that two similar sets of conservation equations are used for the two phases.⁹ Coupling terms appear in the two subsets, representing the exchange of mass, momentum, and energy between the two phases. In both approaches, the equations for the liquid and those for the gas are to be solved simultaneously due to the strong interactions between the two phases.

In the second method, the details of the spray are traded for simplification of the mathematical problem. Otherwise, the second method is equivalent to taking moments of the spray distribution function over the droplet radius and velocity dimensions prior to the integration of the conservation equations over the space and time dimensions instead of after, as in the first method.¹ In this paper, the numerical solution of the spray equation is discussed, but it should not be concluded that the authors have decided that the first approach is superior. The relative advantages and disadvantages of the two procedures are not fully known at present and, therefore, they should both be explored. (Actually, even the derivation of the constitutive equations for the two approaches has yet to be completed for the thick sprays of practical interest.¹)

A statistical description of a spray is made both advisable and adequate by the large number of droplets which constitute it. Such a description is achieved by the use of a distribution function (or probability density function) f which is governed by

$$\frac{\partial f}{\partial t} + \frac{\partial(Rf)}{\partial r} + \nabla_x \cdot (vf) + \nabla_v \cdot (Ff) = \xi \quad (1)$$

Equation (1), which is called the spray equation,⁸ states the principle of conservation of the total number of droplets. The independent variables t, r, x , and v denote time, droplet radius, physical space vector, and velocity space vector, respectively. $R \equiv dr/dt$ and $F \equiv dv/dt$ are the time rate of change of droplet radius and velocity following each droplet and reflect the exchange of mass (vaporization) and momentum (drag) with the surrounding gas. The quantity $f(t, r, x, v) dr dx dv$ is the number of droplets with radius in the range dr around r , with velocity in the range dv around v , which, at time t , are in the volume dx around x . In general, Eq. (1) has eight independent variables. The solutions discussed in this article require six independent variables, having assumed one degree of symmetry in the physical space and no swirl. When a swirling motion is imparted to the gas and/or the liquid, all three velocity components must be accounted for, even in a two-dimensional configuration. This was the case for some of the results presented by Bracco et al.⁴ The source (or sink) term ξ is neglected here, thus disregarding nucleation and secondary breakup of droplets. Such processes may not be entirely negligible near the injector.

The rate of vaporization is expressed as

$$R \equiv \frac{dr}{dt} = -\frac{k}{8\rho r} (1 + 0.3Pr^{1/3} Re^{1/2}) \quad (2)$$

where

$$Re = \rho |u - v| 2r / \mu \quad (3)$$

$$Pr = 4\gamma / (9\gamma - 5) \quad (4)$$

The force per unit mass experienced by a drop can be written as

$$F \equiv \frac{dv}{dt} = \frac{3}{8} \frac{C_D}{r} \frac{\rho}{\rho_L} |u - v| (u - v) \quad (5)$$

where

$$C_D = 24 / Re \quad (6)$$

The scalar form of the spray equation, as integrated herein, is

$$\begin{aligned} \frac{\partial f}{\partial t} + \frac{\partial(Rf)}{\partial r} + \frac{\partial(fv_1)}{\partial x_1} + \frac{\partial(fv_2)}{\partial x_2} + \alpha \frac{fv_2}{x_2} \\ + \frac{\partial(F_1 f)}{\partial v_1} + \frac{\partial(F_2 f)}{\partial v_2} = 0 \end{aligned} \quad (7)$$

where α is equal to 0, 1 for planar and cylindrical coordinates, respectively.

Equations (2) and (5), the droplet vaporization and drag equations, are applicable to thin sprays in which the interdrop distance is much greater than the drop diameter. In this case, droplets do not interfere directly but only through their cumulative effect on the gas. In general, this is not the case in practical combustors in which most of the mass vaporization is likely to occur while the droplets are closely packed and interacting with each other, i.e., in thick sprays.¹ For thick sprays, droplet vaporization and drag equations corresponding to Eqs. (2) and (5) are not presently known. They would include the distribution function itself and therefore they would make the spray equation quasilinear. However, the method of solution discussed in this paper would still be applicable.

IV. Two Formulations

The problem of the unsteady, continuous injection of fuel in the cylindrical chamber of Fig. 2 has been formulated and solved in two different ways. In the first formulation, the continuous arrival of the droplets through the injector exit plane is treated as a boundary condition at the injector exit plane. This is called the boundary value problem. In the second formulation, the continuously injected fuel is discretized in a finite number of parcels. Each parcel is assigned initial values and an initial distribution in space within the combustion chamber. Its time development is then computed by solving the spray equation from the given initial conditions. The behavior of the entire injection is recovered by adding the contributions from the individual parcels. This is called the initial value problem. The initial value formulation was the one adopted in the original computations of combustion of unsteady one-dimensional sprays,² while the more natural boundary value formulation has been used in more recent calculations.⁴⁻⁶

In the boundary value problem, an investigation of the uniqueness condition of the solutions of the hyperbolic Eq. (1) indicates that the required boundary conditions are¹⁰:

$$f(t, r_{\max}, x, v) = 0 \quad (8)$$

$$f(t, r, x, v_{\min}) = 0 \quad (9)$$

$$f(t, r, x, v_{\max}) = 0 \quad (10)$$

$$f(t, r, x_{\text{inj}}, v) = Br^2 e^{-cr} \exp\left(-\left(\frac{v_1 - v_1^*}{d_1}\right)^2\right) \exp\left(-\left(\frac{v_2 - v_2^*}{d_2}\right)^2\right) \quad (11)$$

Equations (8-10) state that there shall be no drops with $r \geq r_{\max}$, $v \leq v_{\min}$, and $v \geq v_{\max}$, respectively.

Equation (11) describes the boundary condition of the spray during the injection at the injector exit plane.

This formulation has an accompanying initial condition

$$f(t=0, r, x, v) = 0 \quad (12)$$

This initial condition states that there are no drops in the chamber prior to injection.

The following condition completely defines an initial value problem for Eq. (1)

$$f(t=0, r, x, v) = Br^2 e^{-cr} \exp - \left(\frac{v_1 - v_1^*}{d_1} \right)^2 \exp - \left(\frac{v_2 - v_2^*}{d_2} \right)^2 \times \exp - \left(\frac{x_1 - x_1^*}{h_1} \right)^2 \exp - \left(\frac{x_2 - x_2^*}{h_2} \right)^2 \quad (13)$$

Equation (13) is similar to Eq. (11), but it specifies the initial distribution function in the entire physical space instead of at the injector exit plane alone. Indeed, as x_1 and x_2 tend to x_1^* , x_2^* , respectively, Eq. (13) tends to Eq. (11) if x_1^* and x_2^* are the coordinates of the center of the injector exit.

Some discussion of the expressions used on the right-hand side of Eqs. (11) and (13) are in order here. These expressions define the spray as it is first formed upon the breakup of the liquid jet or sheet produced by the injector. A knowledge of the breakup process is therefore required to select the expressions. However, such a process is not presently well understood, particularly for the high-injection velocities used in direct injection internal combustion engines.⁷

Accordingly, both the functional forms of the expressions (Nukiyama-Tanasawa in r and Gauss in v_1 and v_2) and their parameters have been selected from scant experimental information and are subject to large errors. Notice, for example, that the expressions of Eqs. (11) and (13) are separable, implying that the initial velocity distribution is independent of the initial drop size; an assumption which cannot be substantiated. The coefficients c , v_1^* , v_2^* , d_1 , d_2 , x_1^* , x_2^* , h_1 , and h_2 are defined and obtained as follows.

Let r_{30} be the volume-number average radius of the droplets as they are first formed.

$$r_{30} \equiv \left[\frac{\int_0^\infty \int_{-\infty}^{+\infty} r^3 f dr dv}{\int_0^\infty \int_{-\infty}^{+\infty} f dr dv} \right]^{1/3} \quad (14)$$

Using the following semiempirical correlation² between r_{30} and r_{inj} (injector radius)

$$r_{30} = ar_{\text{inj}}(We/Re_L)^b, \quad We \equiv \sigma_L/2r_{\text{inj}}\rho v_{\text{inj}}^2, \quad Re_L \equiv 2r_{\text{inj}}\rho_L v_{\text{inj}}/\mu_L \quad (15)$$

where a and b are empirical constants, σ_L , ρ_L , μ_L are the liquid surface tension, specific gravity, and viscosity, respectively; v_{inj} is the injection velocity; and ρ is the gas density at the injector exit. Substituting Eqs. (11) or (13) in (14), it is found that $c = (6)^{1/3}/r_{30}$, where r_{30} is obtained from Eq. (15).

v_1^* and v_2^* are the most probable components of v_1 , v_2 at the injector and d_1 , d_2 define the widths of the velocity distributions. The values of these parameters are somewhat arbitrary at present, since the corresponding detailed knowledge of the atomization process is missing.

Additional parameters appearing in Eq. (13) are x_1^* , x_2^* , h_1 , and h_2 . They play the same role in the physical space as played by v_1^* , v_2^* , d_1 , and d_2 , respectively, in the velocity space. The values of these additional parameters are also somewhat arbitrary.

$B = B(t)$ of Eq. (11) is a factor determined by the conservation of fuel mass through the injector and related to the total number of drops for unit volume. The discussion of the coefficient B for Eq. (13) is postponed to a later section. In Eqs. (11) and (13), $B = 0$, as fuel injection ends.

V. Finite-Difference Scheme

When solved numerically, both the initial and the boundary value problems were solved by the same time-explicit, first-order accurate, upwind differencing, or donor cell differencing scheme.

For example, the finite differencing of the derivative $(\partial(F_1 f)/\partial v_1)$ may be expressed in the following two ways:

$$\frac{\partial(F_1 f)}{\partial v_1} = \left[F_1(v_{1t+1/2})f(v_{1t}) - F_1(v_{1t-1/2})f(v_{1t-1}) \right] / \Delta v_1 \quad \text{for } v_1 < u_1 \quad (16a)$$

$$\frac{\partial(F_1 f)}{\partial v_1} = \left[F_1(v_{1t+1/2})f(v_{1t+1}) - F_1(v_{1t-1/2})f(v_{1t}) \right] / \Delta v_1 \quad \text{for } v_1 > u_1 \quad (16b)$$

Equation (16a) is used when the droplet velocity is smaller than the local gas velocity, so that the droplet is accelerating and hence this finite-difference form of the derivative at v_{1t} emphasizes f corresponding to v_{1t-1} . In Eq. (16b) the droplet is decelerating; therefore, f at v_{1t+1} is used. Note that, in both cases, F_1 is evaluated at the same half-mesh points.

For the present formulation in which the gas is motionless, $v > u = 0$, (i.e., the droplets are moving toward larger values of x_1 and x_2 at all times) and the liquid is without swirl, the finite-difference form of Eq. (7) is:

$$\begin{aligned} f(r_i, x_{1j}, x_{2k}, v_{1t}, v_{2m}, t_2) = & f(r_i, x_{1j}, x_{2k}, v_{1t}, v_{2m}, t_1) + \frac{\Delta t}{\Delta r} \left\{ f(r_i, x_{1j}, x_{2k}, v_{1t}, v_{2m}, t_1) R(r_{i-1/2}) \right. \\ & \left. - f(r_{i+1}, x_{1j}, x_{2k}, v_{1t}, v_{2m}, t_1) R(r_{i+1/2}) \right\} + v_{1t} \frac{\Delta t}{\Delta x_1} \left\{ f(r_i, x_{1j-1}, x_{2k}, v_{1t}, v_{2m}, t_1) - f(r_i, x_{1j}, x_{2k}, v_{1t}, v_{2m}, t_1) \right\} \\ & + \frac{v_{2m}}{x_{2k}^\alpha} \frac{\Delta t}{\Delta x_2} \left\{ x_{2k-1}^\alpha f(r_i, x_{1j}, x_{2k-1}, v_{1t}, v_{2m}, t_1) - x_{2k}^\alpha f(r_i, x_{1j}, x_{2k}, v_{1t}, v_{2m}, t_1) \right\} \\ & + \frac{\Delta t}{\Delta v_1} \left\{ f(r_i, x_{1j}, x_{2k}, v_{1t}, v_{2m}, t_1) F_1(v_{1t-1/2}) - f(r_i, x_{1j}, x_{2k}, v_{1t+1}, v_{2m}, t_1) F_1(v_{1t+1/2}) \right\} \\ & + \frac{\Delta t}{\Delta v_2} \left\{ f(r_i, x_{1j}, x_{2k}, v_{1t}, v_{2m}, t_1) F_2(v_{2m-1/2}) - f(r_i, x_{1j}, x_{2k}, v_{1t}, v_{2m+1}, t_1) F_2(v_{2m+1/2}) \right\} \end{aligned} \quad (17)$$

where

$$r_i = r_{\min} + (i-1)\Delta r \quad i=1,2,\dots,I$$

$$x_{1j} = (j-1)\Delta x_1 \quad j=1,2,\dots,J$$

$$x_{2k} = (k-1)\Delta x_2 \quad k=1,2,\dots,K$$

$$v_{1\ell} = v_{1\min} + (\ell-1)\Delta v_1 \quad \ell=1,2,\dots,L$$

$$v_{2m} = v_{2\min} + (m-1)\Delta v_2 \quad m=1,2,\dots,M$$

$$t_2 = t_1 + \Delta t$$

By this numerical scheme, the distribution function is determined at the advanced time $t + \Delta t$, knowing it at t .

A Taylor series expansion of all terms appearing in Eq. (17), about a point in the six-dimensional space, yields the magnitude of the truncation error at that point.

$$\begin{aligned} \text{Truncation error} = & \frac{\Delta t}{2} \left[\Delta t f_{tt} + \Delta r (f_r R_r + f_{rr} R) \right. \\ & - v_1 \Delta x_1 f_{x_1 x_1} - v_2 \Delta x_2 (f_{x_2 x_2} + 2f_{x_2/x_2}) \\ & + \Delta v_1 (f_{v_1} F_{1v_1} + F_{1v_1} f_{v_1 v_1}) + \Delta v_2 (f_{v_2} F_{2v_2} + f_{2v_2} v_2) \left. \right] \\ & + \text{higher order terms} \end{aligned} \quad (18)$$

where the subscripts of f , R , F_1 , and F_2 indicate partial derivatives evaluated at the same point. Reference to Eq. (18) will be made later in the paper.

VI. Typical Results of the Boundary Value Problem

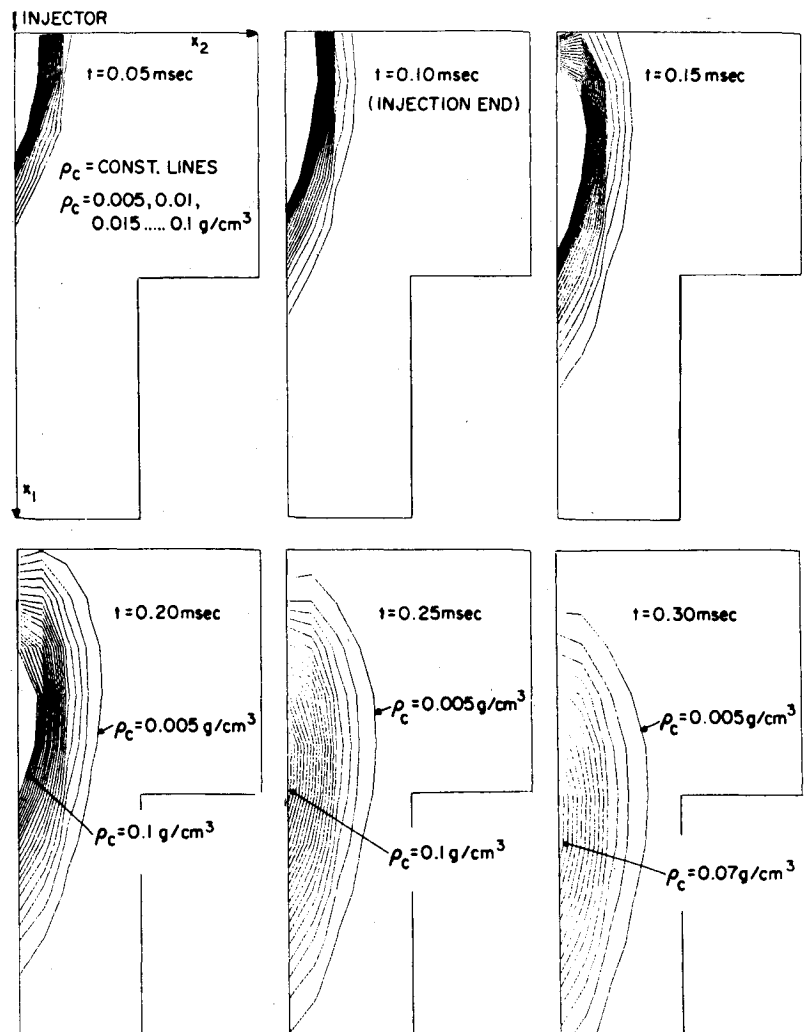
Results of the boundary value problem were reported earlier with emphasis on their possible engineering applications.⁴⁻⁶ One such set of results is given in Fig. 3 and is included in this paper for the sake of completeness. They pertain to the engine configuration of Fig. 2 and were obtained solving Eq. (7), with boundary and initial conditions Eqs. (8-12), by the finite differencing scheme of Eq. (17). In this formulation, the continuous injection is treated by specifying the distribution function at the injector exit plane as a boundary condition in terms of t , r , v_1 , and v_2 . These results were obtained using the following gas-phase properties: $u=0$; $\rho=16.0 \rho_{\text{air}}$; $T=2.64 T_{\text{air}}$; $p=42.0 p_{\text{air}}$; $\mu=3.8 \times 10^{-4}$ g/cm s. Other parameters used included: $a=6.6$; $b=0.2$; $\sigma_L=28$ dyne/cm; $\rho_L=0.8$ g/cm³; $r_{\text{inj}}=250 \mu=250 \times 10^{-4}$ cm; $\mu_L=2.2 \times 10^{-2}$ g/cm s; $\alpha=1$ (cylindrical coordinates); $k=10^{-4}$ g/cm s; $D_2=7.62$ cm; $\gamma=1.35$; $v_{\text{inj}}=15,000$ cm/s. The selected domains for r and v spaces were $10 \mu \leq r \leq 140 \mu$; $0 \leq v_1 \leq 20,000$ cm/s; $0 \leq v_2 \leq 6000$ cm/s.

The results are presented in terms of the "condensed phase density" ρ_c which gives the local and instantaneous amount of mass of liquid fuel per unit volume of combustion chamber.¹

$$\rho_c(x, t) = \int_v \int_r \frac{4}{3} \pi r^3 \rho_L f(t, r, x, v) dr dv \quad (19)$$

The results of Fig. 3 are for a spray for which injection lasts only 0.10 ms (for all results, time is counted from the beginning of injection) and the liquid fuel is shown to

Fig. 3 Boundary value formulation. Calculated time and space variation of condensed phase density in the configuration of Fig. 2.



penetrate and expand into the combustion chamber. In the inner core, where there are no lines, ρ_c is greater than 0.1 g/cm^3 . At first, this core is seen to increase in size and to penetrate quickly due to the continuous addition of fuel, up to $t = 0.1 \text{ ms}$, and to the inertia of the initially large drops. Later the core decreases in size and penetrates slowly due to the continuous vaporization of the drops, which reduces the amount of liquid fuel, and to the smaller inertia of the drops which are now of smaller size (the velocity of a drop tends to the local gas velocity, in this case zero, as its size tends to zero). Notice that the tip of the spray penetrates much more than its core. This is due to the size and velocity of the drops being distributed. Thus, even though the injection velocity is $15,000 \text{ cm/s}$, some drops have axial velocities as high as $20,000 \text{ cm/s}$. Similarly, even though the initial mass-mean drop radius is 45μ , the radius of some drops is as large as 140μ . For additional, similar results, and for more information on their implications for engine combustion, Refs. 2-6 may be consulted.

VII. Initial Value Problem

An initial value problem is now studied. A numerical solution and a closed-form solution are found and compared to investigate the error of the numerical solution. It is concluded that this error can be maintained within acceptable limits.

In the next section it is further shown that the same numerical scheme can be used to give solutions for both the initial value problem and the boundary value problem and that the two numerical solutions indeed coincide within the accuracy of the numerical computations.

Hence the numerical error of the boundary value formulation can also be maintained within acceptable limits, and these limits can be studied by setting up and solving a corresponding initial value problem.

The long way about investigating the numerical accuracy of boundary value formulations, which are more attractive for practical applications, was necessitated by our inability to obtain closed-form solutions for the boundary value problems, whereas we were able to obtain a closed-form solution for the corresponding initial value problem.

In order to reduce a continuous injection to an initial value problem, the continuous injection is divided into discrete parcels of fluid, broken up into drops, and distributed within a small volume by the injector, which are then treated as separate sprays with their initial conditions and their subsequent histories. The behavior of the actual spray due to the continuous injection is reconstructed by numerically summing the individual contributions of all the discretized sprays. This was the approach followed by Bracco² who discretized an unsteady, one-dimensional continuous spray into a finite number of discrete, monodisperse sprays. The present

discretization differs in that the problem is two-dimensional, the discrete sprays remain polydisperse, and, more importantly, the sum of infinitely many discrete sprays is represented by an integral which gives the net effect of the continuous injection.

For the initial value problem, the expressions used for R and F are:

$$R = \chi/r \quad (20)$$

$$F = (\phi/r^2)(u-v) \quad (21)$$

With the preceding expressions for R and F , with χ and ϕ constant, and keeping the assumption that the gas is not changed by the presence of the liquid, the solution of the initial value problem can be obtained analytically except for a final integral in one dimension, time, which will be evaluated numerically.

Equation (7) with the initial conditions of Eq. (13) constitutes a Cauchy problem which can be expressed by an equivalent system of ordinary differential equations

$$\begin{aligned} \frac{dt}{I} = \frac{dx_1}{v_1} = \frac{dx_2}{v_2} = \frac{dr}{R} = \frac{dv_1}{F_1} = \frac{dv_2}{F_2} \\ = \frac{df}{-f\left(\frac{\partial R}{\partial r} + \frac{\partial F_1}{\partial v_1} + \frac{\partial F_2}{\partial v_2} + \frac{\alpha v_2}{x_2}\right)} = ds \end{aligned} \quad (22)$$

In the preceding seven ordinary differential equations, the dependent variables t, x_1, x_2, r, v_1, v_2 , and f can be considered functions of s and of seven independent parameters: $t_0, x_{10}, x_{20}, r_0, v_{10}, v_{20}$, and f_0 . However, setting $t_0 = 0$ at $s = 0$, Eq. (13) gives f_0 in terms of the other parameters.

$$\begin{aligned} f_0(0, r_0, x_{10}, x_{20}, v_{10}, v_{20}) = Br_0^2 e^{-\alpha r_0} \exp\left(-\frac{(v_{10} - v_1^*)^2}{d_1}\right) \\ \times \exp\left(-\frac{(v_{20} - v_2^*)^2}{d_2}\right) \exp\left(-\frac{(x_{10} - x_1^*)^2}{h_1}\right) \exp\left(-\frac{(x_{20} - x_2^*)^2}{h_2}\right) \end{aligned} \quad (23)$$

After solving the seven ordinary differential equations, f vs t, x_1, x_2, r, v_1, v_2 is obtained by eliminating the independent parameters. This elimination is allowed for a nonvanishing Jacobian

$$\frac{\partial(t, r, x_1, x_2, v_1, v_2)}{\partial(s, r_0, x_{10}, x_{20}, v_{10}, v_{20})}$$

Thus, obtaining

$$\begin{aligned} f(t, r, x_1, x_2, v_1, v_2) = B(r^2 - 2\chi t)^{1 - \frac{\psi}{2\chi}} r^{\frac{\psi}{\chi}} e^{-\alpha(r^2 - 2\chi t)^{1/2}} \exp\left\{-\frac{u_1 + (v_1 - u_1)\left(\frac{r^2}{r^2 - 2\chi t}\right)^{\phi/2\chi} - v_1^*}{d_1}\right\}^2 \\ \times \exp\left\{-\frac{u_2 + (v_2 - u_2)\left(\frac{r^2}{r^2 - 2\chi t}\right)^{\phi/2\chi} - v_2^*}{d_2}\right\}^2 \exp\left\{-\frac{x_1 - u_1 t - \frac{(v_1 - u_1)r^{\phi/\chi}}{2\chi - \phi} [(r^2)^{1-\phi/2\chi} - (r^2 - 2\chi t)^{1-\phi/2\chi}] - x_1^*}{h_1}\right\}^2 \\ \times \exp\left\{-\frac{x_2 - u_2 t - \frac{(v_2 - u_2)r^{\phi/\chi}}{2\chi - \phi} [(r^2)^{1-\phi/2\chi} - (r^2 - 2\chi t)^{1-\phi/2\chi}] - x_2^*}{h_2}\right\}^2 \\ \times \left[x_2 - u_2 t - \frac{(v_2 - u_2)r^{\phi/\chi}}{2\chi - \phi} ((r^2)^{1-\phi/2\chi} - (r^2 - 2\chi t)^{1-\phi/2\chi})\right] / x_2 \end{aligned} \quad (24)$$

where

$$\psi = 2\phi + \chi \quad (25)$$

Having solved for f for a discrete spray, a parameter τ_i is introduced such that the i th discrete spray is injected into the chamber at $t = \tau_i$ ($= i\Delta\tau$) where $\Delta\tau$ is the time interval between two subsequent discrete sprays. The distribution function f_i at $t \geq \tau_i$ for this i th discrete spray is obtained simply by replacing t with $(t - \tau_i)$ in Eq. (24).

$$\begin{aligned} f_i(t, r, x_1, x_2, v_1, v_2, \tau_i) = & B \left(r^2 - 2\chi(t - \tau_i) \right)^{1 - \frac{\psi}{2\chi}} r^{\frac{\psi}{\chi}} e^{-c(r^2 - 2\chi(t - \tau_i))^{1/2}} \\ & \times \exp - \left\{ \frac{u_1 + (v_1 - u_1) \left(\frac{r^2}{r^2 - 2\chi(t - \tau_i)} \right)^{\phi/2\chi} - v_1^*}{d_1} \right\}^2 \exp - \left\{ \frac{u_2 + (v_2 - u_2) \left(\frac{r^2}{r^2 - 2\chi(t - \tau_i)} \right)^{\phi/2\chi} - v_2^*}{d_2} \right\}^2 \\ & \times \exp - \left\{ \frac{x_1 - u_1(t - \tau_i) - \frac{(v_1 - u_1)r^{\phi/\chi}}{2\chi - \phi} [(r^2)^{1-\phi/2\chi} - (r^2 - 2\chi(t - \tau_i))^{1-\phi/2\chi}] - x_1^*}{h_1} \right\}^2 \\ & \times \exp - \left\{ \frac{x_2 - u_2(t - \tau_i) - \frac{(v_2 - u_2)r^{\phi/\chi}}{2\chi - \phi} [(r^2)^{1-\phi/2\chi} - (r^2 - 2\chi(t - \tau_i))^{1-\phi/2\chi}] - x_2^*}{h_2} \right\}^2 \\ & \times \left[x_2 - u_2(t - \tau_i) - \frac{(v_2 - u_2)r^{\phi/\chi}}{2\chi - \phi} ((r^2)^{1-\phi/2\chi} - (r^2 - 2\chi(t - \tau_i))^{1-\phi/2\chi}) \right] / x_2 \end{aligned} \quad (26)$$

Here, we digress briefly to determine the coefficient B of Eq. (13). B is found by equating the mass associated with all the droplets of i th discrete spray to the mass injected during the time $\Delta\tau$.

$$\int_r \int_x \int_v \frac{4}{3} \pi r^2 \rho_L f_i(t = \tau_i, r, x_1, x_2, v_1, v_2) dr dx dv = \dot{W}_F \Delta\tau \quad (27)$$

where \dot{W}_F is the mass rate of injection of liquid through the injector. Eliminating f_i between Eqs. (26) and (27) one obtains an expression for B

$$B(t) = (\dot{W}_F(t) \Delta\tau) / \int_r \int_x \int_v \frac{4}{3} \pi r^3 \rho_L \frac{1}{B} f_i(t = \tau_i, r, x_1, x_2, v_1, v_2) dr dx dv \equiv B_i \Delta\tau \quad (28)$$

The distribution function of the continuous spray can now be constructed summing the f_i 's due to all discrete sprays (the total number of which, say, is L)

$$f(t, r, x_1, x_2, v_1, v_2) = \sum_{i=1}^L f_i(t, r, x_1, x_2, v_1, v_2) \quad (29)$$

The summation is allowed because the governing equation is linear. Using Eqs. (26) and (28) and taking the limit for $L \rightarrow \infty$ or $\Delta\tau \rightarrow 0$, Eq. (29) gives

$$\begin{aligned} f(t, r, x_1, x_2, v_1, v_2) = & \int_{\tau=0}^t B_\tau \left(r^2 - 2\chi(t - \tau) \right)^{1 - \frac{\psi}{2\chi}} r^{\frac{\psi}{\chi}} e^{-c(r^2 - 2\chi(t - \tau))^{1/2}} \\ & \times \exp - \left\{ \frac{u_1 + (v_1 - u_1) \left(\frac{r^2}{r^2 - 2\chi(t - \tau)} \right)^{\phi/2\chi} - v_1^*}{d_1} \right\}^2 \exp - \left\{ \frac{u_2 + (v_2 - u_2) \left(\frac{r^2}{r^2 - 2\chi(t - \tau)} \right)^{\phi/2\chi} - v_2^*}{d_2} \right\}^2 \\ & \times \exp - \left\{ \frac{x_1 - u_1(t - \tau) - \frac{(v_1 - u_1)r^{\phi/\chi}}{2\chi - \phi} [(r^2)^{1-\phi/2\chi} - (r^2 - 2\chi(t - \tau))^{1-\phi/2\chi}] - x_1^*}{h_1} \right\}^2 \\ & \times \exp - \left\{ \frac{x_2 - u_2(t - \tau) - \frac{(v_2 - u_2)r^{\phi/\chi}}{2\chi - \phi} [(r^2)^{1-\phi/2\chi} - (r^2 - 2\chi(t - \tau))^{1-\phi/2\chi}] - x_2^*}{h_2} \right\}^2 \\ & \times \left[x_2 - u_2(t - \tau) - \frac{(v_2 - u_2)r^{\phi/\chi}}{2\chi - \phi} ((r^2)^{1-\phi/2\chi} - (r^2 - 2\chi(t - \tau))^{1-\phi/2\chi}) \right] / x_2 d\tau \end{aligned} \quad (30)$$

The preceding time integral, known as a convolution integral, cannot be evaluated in closed form. However, its numerical evaluation can be made much more accurate than the numerical solution of the original spray equation with its six independent variables, by using higher order schemes and smaller time increments. Hence, we call the numerical evaluation of Eq. (30) the "analytical" solution of the initial value problem.

In practice, the $\Delta\tau$ used for the integral of the initial value problem was one-half the Δt used for the differential equation of the corresponding boundary value problem and a second-order scheme was employed for the integral, whereas, as previously mentioned, a first-order donor cell differencing scheme was adopted for the differential equation.

VIII. Numerical Accuracy

The results of Figs. 4-6 pertain to the engine configuration of Fig. 2 and were obtained with the same computational parameters as those of Fig. 3 (given in Sec. VI). They are analytical and numerical results of the initial value problem. Droplet distribution functions vs droplet radii are given of those droplet which have no radial velocity ($v_2 = 0$) and an axial velocity (v_1) of 4000 cm/s at the injector location (point $x_1 = x_2 = 0$ of Fig. 2) and at the indicated times after the beginning of the injection. The initial conditions are the same for both analytical and numerical results. Figure 4 shows that the numerical error for the smaller droplets is already significant after one $\Delta t = 10^{-5}$ s. Figure 5 shows the numerical error to be significant for all drop sizes after $10 \Delta t$ s.

The numerical results with large errors were obtained with relatively few mesh points: 9, 9, 6, 5, and 5 for the x_1 , x_2 , r , v_1 , and v_2 dimensions, respectively.

The expression for the truncation error, Eq. (18), indicates that the error should be reduced by a factor of 4 if the number of mesh points for all six independent variables is doubled, as one would expect for a first-order scheme. This is assuming that all the derivatives appearing in Eq. (18) are of order 1 when dependent and independent variables are properly scaled.

Figures 4 and 5 show that the factor of 4 reduction in error is verified for large drops but not for small drops. Moreover, the doubling of the mesh points for all six independent variables results in an increase of the computation time by approximately a factor of $2^6 = 64$.

To avoid unnecessary increases in computational time, the remainder term of the first-order scheme can be studied to

isolate the second-order derivatives which contribute most of the numerical error. Then the number of mesh points can be selectively increased.

For our physical configuration, with steady injection into a stationary gas, it is likely that the sharpest gradients are to be found near the injector. One can then use the initial condition of the distribution function, Eq. (13), to calculate explicitly all the necessary derivatives. For the selected initial condition, it is found that the derivatives in the r , v_1 , and v_2 spaces contribute most of the error and that the smaller drops are indeed affected more than the larger ones. In terms of the truncation error expression of Eq. (18), the second, fifth, and sixth terms are the larger of the last six terms in the given

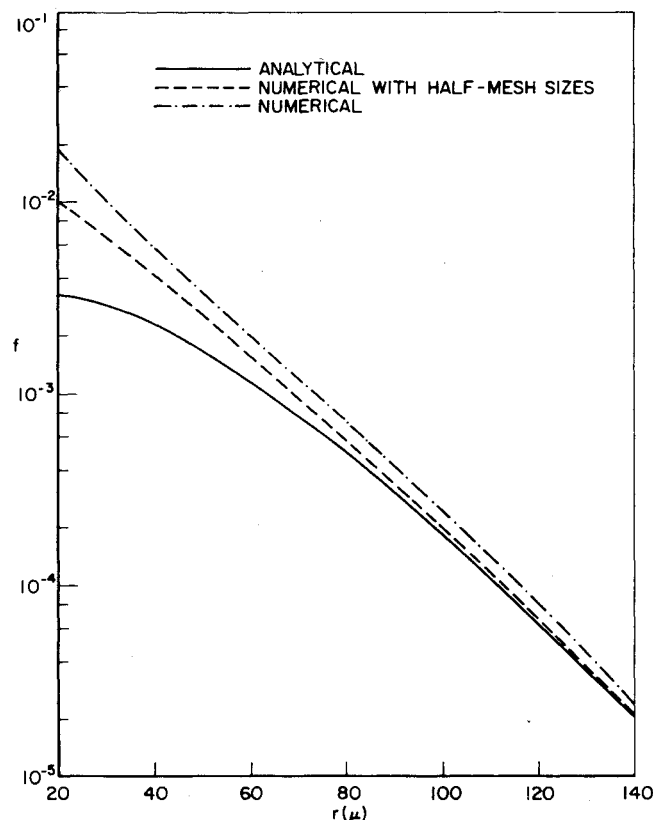


Fig. 5 f vs r for $t = 10^{-4}$ s, $x_1 = 0$, $x_2 = 0$, $v_1 = 4000$ cm/s, $v_2 = 0$.

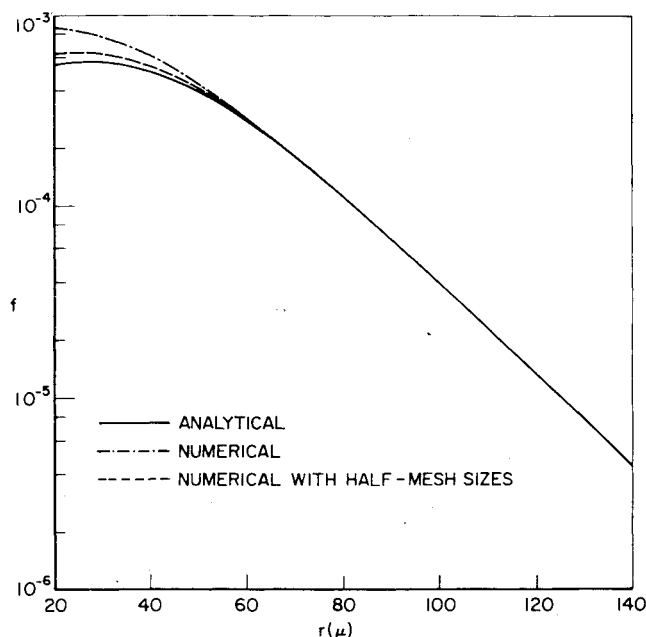


Fig. 4 f vs r for $t = 10^{-5}$ s, $x_1 = 0$, $x_2 = 0$, $v_1 = 4000$ cm/s, $v_2 = 0$.

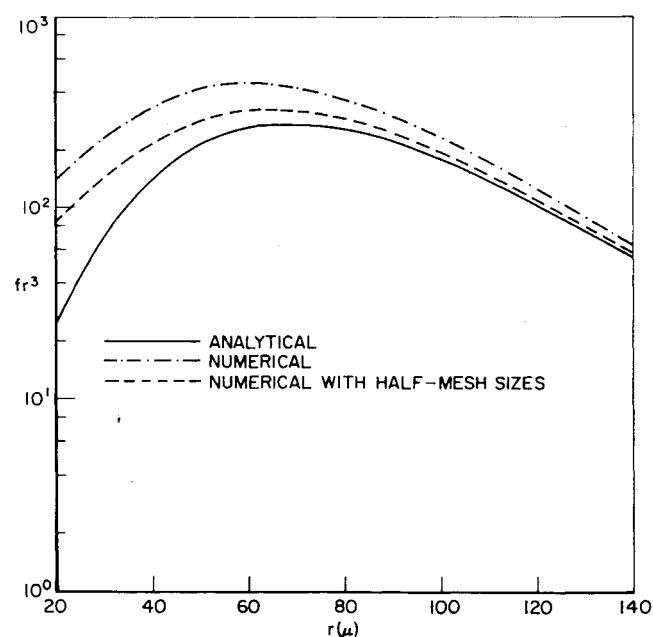


Fig. 6 fr^3 vs r for $t = 10^{-4}$ s, $x_1 = 0$, $x_2 = 0$, $v_1 = 4000$ cm/s, $v_2 = 0$.

order. Accordingly, the same numerical error is found using 9, 9, 12, 9, 7 mesh points for the x_1 , x_2 , r , v_1 , v_2 dimensions as by doubling the number of all mesh points indiscriminately. The computational time is then increased by a factor of 10 instead of 64. Even so, the computation time per time cycle is 0.75s on an IBM 360/91. With $\Delta t = 5 \cdot 10^{-6}$ s, 4.5 ms of real-time spray activity can be computed in 15 min of computer time.

The order of magnitude of the time increment was selected on physical grounds so as to respect the inequalities: $v_1 \Delta t < \Delta x_1$, $v_2 \Delta t < \Delta x_2$, $F_1 \Delta t < \Delta v_1$, $F_2 \Delta t < \Delta v_2$, and $R \Delta t < \Delta r$.

As previously stated, the numerical scheme employed is time explicit, first-order accurate in all spaces and time and has upwind differencing. Although upwind differencing has good numerical stability properties, it is first-order accurate and causes significant numerical inaccuracy due to numerical diffusion. Center differencing in all spaces could be used to increase the numerical accuracy, and implicitness⁵ in time could be incorporated to achieve numerical stability. An implicit scheme was not used for fear of large computer storage requirements to keep the distribution function at two time levels in its five dimensions. This requirement may be reduced significantly by appropriate, more sophisticated programming.

In any case, the numerical error of interest for applications to internal combustion engines is not the largest in the field but that affecting that family of drops whose fuel mass is the largest. Since the mass of a drop goes as r^3 , the family of drops containing the largest mass is found by considering fr^3 , as in Fig. 6, which shows that most of the mass is contained in droplets with $r = 70 \mu \pm 30 \mu$. Wanting to increase the accuracy of the numerical solution uniformly, nonuniform grid spacing could be used to increase the accuracy of the computations for the smaller drops.

The physical problem which has been considered is unusually simple, having treated the gas as unaffected by the spray and having used Eqs. (20) and (21) for the droplet vaporization and drag.

However, the approach is likely to be useful in more complex and practical cases as well. If a computer program is developed for more comprehensive and realistic cases, the same program can also be used for a test run employing the simplified configuration which allowed us to obtain a closed-form solution. Satisfactory comparison of the analytical and numerical results of the simplified case would then become a necessary condition even though it cannot be proved to be a sufficient one.

Finally, the same case was numerically solved both as a boundary value problem and as an initial value problem with the two solutions agreeing. However, the initial conditions for the initial value problem was not arbitrary, but rather the solution of the corresponding boundary value problem at $t = 5 \cdot 10^{-6}$ s. That is, for the two solutions to be equivalent, the initial distribution of the fuel in the chamber, which results from the dispersion of the first discretized parcel of fuel, cannot be selected independently of the boundary condition at the nozzle exit plane; an integration of the boundary value problem must be carried out through the time during which the discretized parcel is injected to establish a compatible initial condition for the initial value problem.

IX. Conclusions

The numerical computation of the propagation and vaporization of a two-dimensional unsteady spray in a gas was considered. The approach followed was to use the spray equation to represent the evolution of the spray, instead of the basically equivalent approach of using two coupled sets of similar conservation equations for the two phases. The problem was formulated both as a boundary value problem and an initial value problem. In the boundary value problem, the continuous arrival of the droplets through the injector exit plane is treated as a boundary condition at the injector exit

plane. In the initial value problem, the continuously injected fuel is discretized in a finite number of parcels. Each parcel is assigned initial values and an initial distribution in space within the combustion chamber. The time development of each parcel is then computed by solving the spray equation from its given initial conditions. The behavior of the entire injection is recovered by adding the contributions from the individual parcels. The boundary value formulation is more convenient for applications, but the initial value formulation yielded an analytical solution which is very useful for the evaluation of numerical errors. Numerical solutions to both formulations were obtained using the same time-explicit, first-order accurate, upwind difference scheme and typical results of both formulations were presented. When the same case was numerically solved, both as a boundary value problem and an initial value problem, the two solutions agreed, thus proving the equivalence of the two formulations.

It was thus concluded that the selected numerical scheme can yield acceptably accurate results for the physical configurations studied with computation times of the order of 10 min on an IBM 360/91. Even though the physical configurations considered are realistic for direct injection, internal combustion engines, the model used is not. Therefore, the results are of limited practical value.

However, the analytical solution used to evaluate the numerical errors can be used to assess the errors of more comprehensive and realistic models by just applying them to the simple cases for which the analytical solution is valid. Such an exercise is highly recommended as the evaluation of numerical errors is otherwise a difficult task.

Acknowledgments

Some of the results of this paper were presented at the 5th International Colloquium of Gas Dynamics of Explosions and Reactive Systems, University of Orleans, Bourges, France, September 1975 or at the Fall Meeting of The Combustion Institute Eastern States Section, Drexel University, Philadelphia, Pa., November 1976. The authors are indebted to C. K. Westbrook, Lawrence Livermore Laboratory, Livermore, Calif., who suggested the boundary value approach and made other valuable inputs. The work was carried out under NSF Grants AER 74-21220 and 75-09538, D. Senich, Grant Monitor, and DOE Contract EC-77-S-02-4191, J. Birkeland, Contract Monitor.

References

- ¹ Bracco, F. V., "Introducing a New Generation of More Detailed and Informative Combustion Models," *SAE Transactions*, Vol. 84, 1975, pp. 3317-3340.
- ² Bracco, F. V., "Theoretical Analysis of Stratified, Two-Phase Wankel Engine Combustion," *Combustion Science and Technology*, Vol. 8, Nos. 1 and 2, Oct. 1973, pp. 69-84.
- ³ Reitz, R. D. and Bracco, F. V., "Studies Toward Optimal Charge Stratification in a Rotary Engine," *Combustion Science and Technology*, Vol. 12, Nos. 1-3, Jan. 1976, pp. 63-74.
- ⁴ Bracco, F. V., Gupta, H. C., Krishnamurthy, L., Santaviceca, D. A., Steinberger, R. L., and Warshaw, V., "Two-Phase, Two-Dimensional Unsteady Combustion in Internal Combustion Engines: Preliminary Theoretical-Experimental Results," Paper 760114, SAE 1976 Congress, Feb. 1976.
- ⁵ Westbrook, C. K., "Three-Dimensional Numerical Modeling of Liquid Fuel Sprays," *The Sixteenth Symposium on Combustion*, The Combustion Institute, Pittsburgh, Pa., 1977.
- ⁶ Haselman, L. C. and Westbrook, C. K., "A Theoretical Model for Fuel Injection in Stratified Charge Engine," Paper 780318, SAE 1978 Congress, Feb. 1978.
- ⁷ Reitz, R. D. and Bracco, F. V., "Breakup Regimes of a Single Liquid Jet," Combustion Institute Eastern States Section Fall Meeting, Paper No. 12, Nov. 1976.
- ⁸ Williams, F. A., *Combustion Theory*, Addison-Wesley, Reading, Mass., 1965.
- ⁹ Harlow, F. H. and Amsden, A. A., "Numerical Calculations of Multiphase Fluid Flow," *Journal of Computational Physics*, Vol. 17, Jan. 1975, pp. 19-52.
- ¹⁰ Courant, R. and Hilbert, D., *Methods of Mathematical Physics*, Vol. II, Interscience Publishers, N.Y., 1966.